A Semi-Empirical Model for Transverse Weld Deflections of Square Tubular Automotive Beams

Analytic model is simplified to run on a PC so quick answers can be had in the design state

BY E. F. RYBICKI, G. L. NAGEL, R. B. STONESIFER, AND E. G. MILLER

ABSTRACT. The fabrication process for automobile frames requires tolerances in locating attachment points. One joining process that can affect the location of reference points is arc welding. Thus, it is important to understand the relation between the geometry of the frame, the welding parameters and the deflections introduced by welding.

Automobile frame members and joint configurations have complex geometries and contain numerous welds. The ultimate objective of studies such as this one is to develop guidelines and simple analytical models that can be used for controlling weld deflections in complex frames. This paper describes a combined experimental and analytical approach to developing a model for predicting and better understanding weld deflections resulting from gas metal arc welding (GMAW) on simple tubular beam geometries.

A semi-empirical model is developed based on a combination of assumed physical behavior and data. The model has two empirical parameters which are evaluated from data. This two parameter model was able to predict deflections for 45 welding experiments using a variety of beam sizes, weld lengths and weld heat inputs with the majority of predictions being within ±5% of the measured values. All but four predictions were within ±10%.

Having established the accuracy of the model, it was then used to examine the effects of variables such as weld length, heat input, beam height, beam size, and wall thickness on weld deflections. Results are presented in graphical form to show trends.

E. F. RYBICKI is with The University of Tulsa, Tulsa, Oklahoma, G. L. NAGEL and E. G. MILLER are with General Motors Technical Center, Warren, Michigan, and R. B. STONESIFER is with Computational Mechanics Inc., Julian, Pennsylvania.

KEY WORDS

Modeling
GMAW
Tubular Beams
Automobile Frames
Distort. Prediction
Deflect. Prediction
Transverse Welds
Beam Geometry
Weld Parameters
Semi-Empirical Model

Introduction

Initial design stages for automotive frames often require a capability to quickly evaluate several alternative frame and frame joint designs. Factors to be considered include strength, stiffness, cost, ease of fabrication, time to fabricate, and manufacturability. Thin walled tubular beams are commonly used in automobile frames because their high stiffness-to-weight ratios make them cost effective primary load carrying structures. An important aspect of assembling automobile frames is selecting appropriate methods for joining frame members and attaching other components to the frame. For automotive frames, the joining process is generally some form of welding.

Single sided welding methods such as GMAW are used for cases where it is difficult to access interior tube surfaces for spot welding. While offering the advantages of tolerating fit-up variations and being capable of handling galvanized materials, GMAW has the disadvantage of introducing larger weld deflections than other welding processes such as spot welding. Thus, it is important for automobile designers to have a capability for predicting deflections resulting from GMAW.

It is not the intent to conduct a comprehensive review of papers related to

weld deflections for all geometries but to mention a representative group of references related to weld deflections of tubular beams and frames. The concept of predicting weld deflections is not new. Many studies on weld deflections for plate configurations with groove and fillet welds have been done and reported (Ref. 1). Extensive work has been done by Masabuchi and coworkers on weld residual deflections (Ref. 2). Much of this work includes transient temperature analyses and residual deflections, strains, and stresses for plate geometries for a variety of materials. The models show good agreement with data for these configurations. Arya and Parmar (Ref. 3) conducted experiments and developed a model for the effect of weld parameters on angular deflections of CO_2 shielded flux cored arc welding of V-groove plates. The weld parameters investigated were arc voltage, wire feed rate, welding speed and groove angle. The authors concluded that a polynomial containing the following terms fits the data: a constant term, linear terms in all variables, a term of the product of arc voltage times wire feed rate, and a term of arc voltage times welding speed. Kjaersgaard and coworkers (Ref. 4) examined the effect of selected weld parameters on the resulting angular deflections of groove welded plates. The metal was ship steel. Experiments were done to determine the effects of plate thickness, weld sequence, and weld groove geometry on angular rotations. Fillet welds were used to join a stiffener plate to a base plate. The authors found that welding sequence and weld groove geometry could be used to reduce angular deflections.

Ueda and co-workers (Ref. 5) developed a method to predict the deflections of welded deck plate panels. The method is based on identifying the inherent plastic strains remaining in the welded structure due to welding. The inherent strains are inputs for an elastic analysis and weld deflections for related geometries are predicted. Tekriwal and Mazumder (Ref. 6) presented a three-dimensional finite element transient thermomechanical analysis of a gas metal arc weld for groove welding two flat plates. The authors compared transient strain data at points away from the heat affected zone (Ref. 6) with predicted strain values and reported good qualitative agreement. Displacements due to welding were calculated but were not compared with displacement data.

Finite element analyses for deflections of flame forming plates and draw bead welding for distortion control are described (Refs. 7 and 8). While plate and cylinder geometries have been studied, less work has been directed at the deflections due to GMAW of tubular beams. Hou and Tsai (Ref. 9) modeled gas metal arc welding of a planar tubular frame. The frame was made of inch (25.4 mm) square tubing. The model contained a temperature analysis and a one-dimensional elastic-plastic stress analysis. Weld deflections for individual joints were predicted and input to a beam finite element analysis to represent the frame. The authors reported qualitative agreement between the predicted deflections of the model and the measured values.

The necessity for getting quick answers in the preliminary design stage in the automobile industry rules out the use of complex finite element models. Thus, there is a need for a simple model to predict weld induced deflections of tubular structures. The model should represent the important factors in the welding process and be simple enough to run many cases for a comparison basis in a short time. The level of simplicity needed to accomplish this would be attained if the model could be run on a personal computer.

To attain this level of simplicity, the model presented in this paper is semi-empirical in nature. This means that the model includes an analytical portion and an experimentally based portion. The analytical portion is formulated to represent a deformation related mechanism and contains important factors characterizing the weldment. These factors include heat input, weld length, and the cross-section dimensions of the tubular member. Two unknowns enter the analytical formulation as a result of the simple representation of the deformation mechanism. These unknowns, representing the empirical portion of the model, appear in the final equations as unknown coefficients to be determined with the aid of experimental weld deflection data.

While the long range goal of this work is to predict weld deflections in a complex three-dimensional (3D) frame geometry with many welded joints and attachments, the approach is to start with a single weld on beam configuration. The reason is that welded joints and attachments typically involve welds that are parallel or transverse to the axes of the frame members. Hence in developing a capability for predicting weld distortions in frames, it is reasonable to start by developing a model to predict the weld deflections for a single transverse or axial weld on a typical tubular member.

Once the models for single transverse and axial welds are developed, these models can be evaluated for use as building blocks to predict the behavior of more complex welded joint configurations. Finally, a 3D beam finite element model can incorporate the predicted weld joint deflections from the joint models to predict the deformations of frame subassemblies. While the 3D beam model is not the focus of this paper, it is noted that coupling the models for single welds to a 3D frame model will require development and further verification with weld deflections from 3D welded frames.

The focus of this paper is on developing a model to predict the deformations of a single transverse weld. The model is analytical and can be easily programmed on a personal computer using spreadsheet software. A series of experiments was conducted to evaluate the accuracy of the model and to study the behavior of transverse weld deformations. The model was then used, along with the data, to examine the influence of selected welding and geometric parameters on the weld deflections.

Description of the Model

This paper is concerned with the development of a simple model to predict the weld deformations caused by welds that are transverse to the axis of a tubular member. A typical tubular beam is shown in Fig. 1. While this paper is primarily concerned with square beams, the cross-section shown is rectangular with dimensions b x h and thickness, t. The transverse weld (Fig. 1) is transverse to the long axis of the beam and has a length which is less than or equal to the base dimension of the beam (b). Cooling of the weld deposit will cause the end of the beam to move upward as shown in Fig. 1. The transverse weld is made by adding a filler metal as the arc moves across the beam. The heat input (H) is in units of kilojoules per in. The deflection of the beam is measured in terms of the change in slope ($\Delta\Theta$), as shown in Fig. 1, in units of thousandths of an in./ft, referred to below as mils/ft. It is important to note that the analysis presented here is for free end conditions. That is, clamping of the type shown in Fig. 2, where the clamp is far enough away from the weld to not cause local deflections in the weld region.

The mechanism for the model is based on the following experimentally observed behavior. Consider two beams, each with a single transverse weld at mid-length. One beam is clamped at both ends before welding so that 1) no moment is applied to the beam by the clamps before welding, and 2) no deflection of the beam can occur during welding. The other beam is restrained at one end during welding as shown in Fig. 2. When the first beam is welded and then unclamped at one end, its

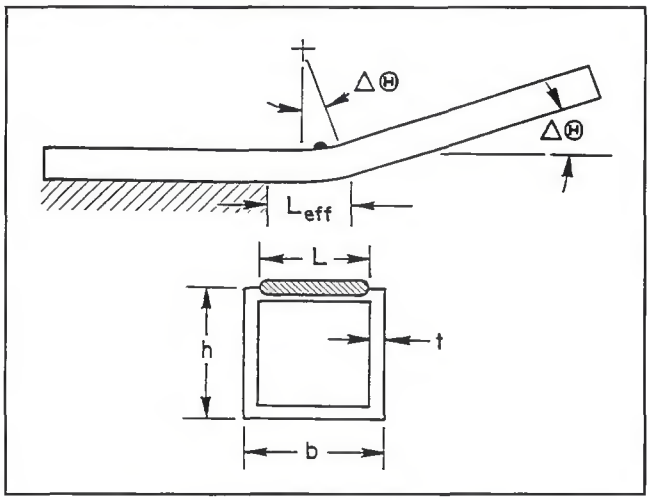

Fig. 1 — Deflection due to a transverse weld on a tubular beam.

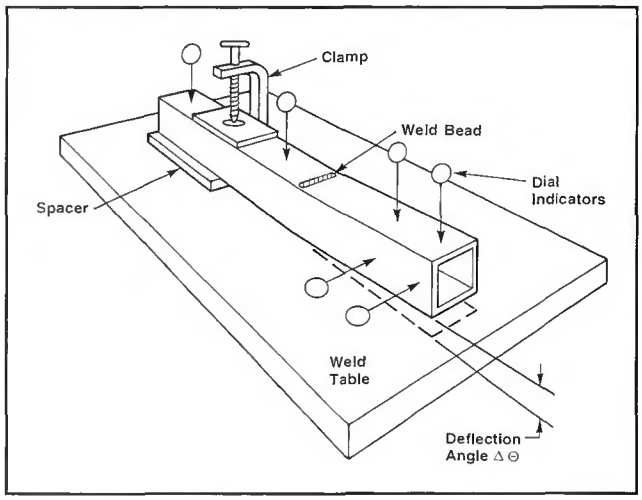

Fig. 2 — Illustration of fixture and dial deflection gages for transverse welded beam.

springback deflection (slope) was found to be about the same as that of the beam restrained at one end during welding. This suggests the final deflection of the beam is elastically related to the moment in the clamped beam after welding but before unclamping. The elastic deflection occurring as a result of releasing this moment is assumed to be equal to the deformation or change in slope, $\Delta\Theta$, shown in Fig. 1.

From beam theory, the curvature of a beam acted on by a moment is equal to M/EI, where M is the moment, E is Young's modulus and I is the moment of inertia of the cross-section. If the moment acts over an effective length along the axis of the beam, denoted by L_{eff} as shown in Fig. 1, then the change in slope over the length L_{eff} is given by

$$\Delta\Theta = (M/EI)\, L_{eff} \qquad (1)$$

An estimate of the moment in the constrained welded beam can be obtained by assuming that the residual stress due to the weld is equal to the yield stress of the material, σ_y. Then the force caused by the residual stress due to the weld is equal to the yield stress times the area over which it acts. The area is assumed to be $t(L + \delta L)$ where δL is a zone of influence outside of the length, L. The moment arm for the force is h/2, where h is the beam height defined in Fig. 1. The equation for the moment in the clamped beam is

$$M = \sigma_y\, t(L + \delta L)\, h/2 \qquad (2)$$

It is assumed that δL is proportional to the heat input, H, divided by the thickness, t

$$\delta L = C_1 (H)/t \qquad (3)$$

where C_1 is an empirical parameter.

Next, an expression for the effective length, L_{eff}, shown in Fig. 1, is developed. It is consistent to assume L_{eff} is proportional to H/t, but the effective length is also expected to depend on the cross-sectional dimensions of the tube such that larger cross-sections have a larger L_{eff}. Because weld residual stresses are self equilibrating and thin-walled tubes are of interest, there is a length over which the effect of the weld induced stresses will attenuate. Thin-shell theory for circular cross sections suggests that the length is proportional to the quantity $\sqrt{Dt}$, where D is the diameter and t is the thickness. Thus, the equation for L_{eff} is assumed to be

$$L_{eff} = C_2 (H/t)\sqrt{Dt} \qquad (4)$$

where C_2 is an empirical parameter. For beams with square cross-sections, b is equal to h and D is assumed to be b or h. While this study is concerned with square beams, there is one weld deflection data point for a rectangular beam. A tubular beam with a rectangular cross-section requires an expression for D in terms of b, h and t. Since such an expression was not readily available, D was set equal to the arithmetic average of b and h for the single rectangular beam.

Substituting Equations 2 – 4 into Equation 1 gives the following expression for $\Delta\Theta$.

$$\Delta\Theta = (\sigma_y t h/2EI)\,(L + C_1 H/t)\, C_2 H \sqrt{(D/t)} \qquad (5)$$

An interesting observation about the assumptions of the model can be made by noting the form of Equation 5. It is noted that C_2 is multiplied by the entire expression. This has the effect of relaxing the assumption made for Equation 2, that the residual stress is equal to the yield stress, to a more general assumption that the residual stress is proportional to the yield stress of the material. The proportionality constant would be unknown and would be incorporated in the empirical parameter C_2 without changing the form of Equation 5.

Only one material is being considered here, so properties such as E and σ_y are not variables and can be included in the empirical parameters. The following empirical parameters are defined to replace C_1 and C_2 in Equation 5

$$C_5 = C_2\, \sigma_y/2E \text{ and}$$
$$C_6 = C_2\, C_1\, \sigma_y/2E \qquad (6)$$

Equation 5 then has the form

$$\Delta\Theta = C_5\, h\, H\, L\, \sqrt{Dt/I} + C_6\, h\, H^2\, \sqrt{D/t/I} \qquad (7)$$

It can be seen from Equations 6 and 7 that the weld deflection or change in slope of the beam depends on the heat input (H), the length of the weld in the direction transverse to the beam (L), the moment of inertia of the beam cross-section (I), the thickness of the beam (t), the distance from the neutral axis to the weld deposit (h/2), the modulus (E) and the annealed yield stress of the material (σ_y).

Determination of the empirical parameters, C_5 and C_6, requires a minimum of two weld deflection experiments using different geometries or heat inputs. Due to variability in experimental weld deflections for a given weld design, a least squares fit using more than two data points is preferable. To show the effectiveness and accuracy of the model for a wide range of welding and geometric parameters requires

experiments over that range of parameters. Because of experimental variability, it is also important that multiple data points be developed for a specific combination of geometric and weld parameters. Such data provide a basis for determining whether differences between predicted deflections and experimental deflections are due to experimental variability or inaccuracy of the model.

The approach selected to evaluate C_5 and C_6 depends on the objective of using the model. For example, if the objective is to evaluate the capability of Equation 7 to predict weld deformations for a variety of weld and geometric parameters, then one approach is to evaluate C_5 and C_6 for a given subset of the data and then use Equation 7 to predict deflections for the remaining experiments involving different weld and geometric parameters.

If this approach indicates that Equation 7 is a reasonable model, the predictive capability of the model over the entire range of geometries and welding parameters can be improved by using a second approach. In this approach, C_5 and C_6 are determined through a least squares fitting of all of the data. Both approaches are used here. First the subset method is used and then the model is fit to all the data. It will be seen that the C_5 and C_6 values resulting from the two approaches are quite similar.

Test Procedure and Equipment

To obtain an understanding of the magnitude and reproducibility of weld deflections for conditions of interest, a series of transverse weld experiments were conducted. A five axis robot in the short circuiting welding mode was used throughout the transverse weld deflection experiments to achieve consistent and repeatable test conditions. Arc weld parameters such as welding current, voltage , wire feed speed, and welding time were measured and recorded for each weld on a weld monitor. Additional welding information such as gas mixture (75% Argon 25% CO_2), travel speed and weld dimensions was recorded separately.

Two deflection measurement methods were examined. The first method required the use of a coordinate measurement machine to measure the X, Y and Z locations of tooling balls, which were adhesively bonded to strategically located points on each specimen. This required the specimen to be removed from the fixture for time consuming preweld and postweld measurements. The second method utilized six battery powered digital indicators positioned in a pattern around the specimen as shown in Fig. 2. This method did not require removal of the test specimen for measurement and allowed real-time data gathering.

The tubular beam test specimen was fixtured and clamped to a rigid welding table with a spacer inserted under the specimen to permit downward deflection during welding. To prevent clamps from distorting the test specimen, a reinforcement plate was inserted under each clamp. Arc weld schedules with high and low heat inputs were developed for both the 0.060 in. and 0.080 in. wall thickness specimens with care taken to avoid melt through. A time of 15 minutes was required for cool-down to allow the specimen deflection to stabilize before final indicator readings were taken.

Welds were done on three square beam sizes and one rectangular beam. A variety of weld conditions were considered. These included transverse welds of different lengths and a range of heat inputs. All welds were done on tubular beams made of one material. The material for the 2.25 × 2.25-in. beams and the 2 × 2-in. beams was ASTM (American Society of Testing Materials) A 513 Class 1 steel. For the 3 × 3-in. and the 3 × 2.-in. beams, the material was ASTM A500 Grade B shaped steel.

Comparison of Predicted Deflections and Data for Transverse Welds

Weld deflection data were obtained for 45 welds. All of these welds were far enough from other transverse welds (more than three times the length of the side of the square tube) so that the deflections were not influenced by residual stress fields of neighboring welds. The data are mainly for tubular beams that are 2.25 × 2.25 × 0.06-in. and 3 × 3 × 0.075-in. There were also three welds for 2 × 2 × 0.075- in. beams and one weld on a 3 × 2 × 0.080-in. beam.

To evaluate the capability of the model to predict the weld deflections, values of C_5 and C_6 were determined from only the data points for the 2.25-in. square beams. Using these values, the weld deflections for the 3-in., the 2-in. and the 3 × 2-in. beams were then predicted. The values of C_5 and C_6, as determined from a least squares fit of data for the 2.25 × 2.25-in. data, are

$$C_5 = 1.3445 \text{ in.}^2/\text{kJ}$$
$$C_6 = 0.003792 \text{ in.}^5/\text{kJ}^2 \quad (8)$$

Table 1 summarizes the welding and geometric parameters for 45 weld distortion experiments and also compares experimental and predicted deflections using the above values of C_5 and C_6. Columns 2 through 5 of Table 1 describe the geometry of the beam. Column 6 is the heat input for the weld. Column 7 is the length of the weld. The last three columns contain the experimental weld deflection, the corresponding predicted value, and the percent difference between the experimental and the predicted values. Looking at the last column of Table 1, it can be seen that the largest percent difference is almost 16% for SWB6L1. The agreement between the model and the data is good, considering the complexity of the physical phenomena and recalling that the data for the 3 × 3-in. beams, the 2 × 2-in. beams and the 3 × 2-in. beam were not used in determining C_5 and C_6. Also, the thicknesses of these beams are different from that of the 2.25 × 2.25-in. beams. To illustrate that experimental variability enters into consideration, note that SWB6L1 and SWB6L2 are largely duplicate specimens but have experimental deflections which differ by more than 20%.

A comparison of the predicted deflections and the experimental deflections, for all beam sizes, is also shown in Fig. 3A through 3D. The closeness of the points to the 45-deg lines shown in Fig. 3 indicates the close agreement between the model and the data.

In order to provide the best overall accuracy for the tested range of weld and geometric parameters, C_5 and C_6 were obtained through a least squares fit to all 45 data points. Doing this, the following values of C_5 and C_6 were obtained

$$C_5 = 1.3123 \text{in.}^2/\text{kJ}$$
$$C_6 = 0.004042 \text{ in.}^5/\text{kJ}^2 \quad (9)$$

Table 2 shows a comparison of the predicted and experimental weld deflections for the above values of C_5 and C_6. The maximum percent difference of 17.3% again occurs for SWB6L1. Figure 4 shows a comparison of the predicted and experimental deflections using the same graphical approach used in Fig. 3. From Fig. 4, it can be seen that most of the data are within ±10% of the predicted values.

Statistical Significance of the C_6 Term in the Model

The magnitude of C_6, as calculated from the data of this study, is much smaller than the magnitude of C_5. A statistical analysis was done to determine whether the data implies that C_6 is essentially zero.

The statistical method used is called a paired t-test. This test determines the certainty with which it can be said that C_6 is not zero for the particular set of data considered. Two versions of the

Table 1 — Transverse Weld Deflection Data and Predicted Deflections from Model Using C5 and C6 from Best Fit of 2.25 × 2.25-in. Data

C5 = 1.3445 $in.^2/kJ$
C6 = 3.792E-03 $in.^5/kJ^2$

Specimen ID	Base (b) (in.)	Height (h) (in.)	Beam thick t, (in.)	Beam moment I, ($in.^4$)	Heat input, H (kJ/in.)	Bead length (in.)	Exp. theta (mpft)	Model theta (mpft)	Diff (%)
SWB6L1	2.250	2.250	0.060	0.420	2.66	2.15	19.0	16.0	−15.7
SWB6L2	2.250	2.250	0.060	0.420	2.76	2.00	15.0	15.5	3.6
SWB6H1	2.250	2.250	0.060	0.420	4.40	2.00	25.0	25.7	2.8
SWB6H2	2.250	2.250	0.060	0.420	4.43	2.10	27.0	27.0	0.2
SWB8L1	2.000	2.000	0.080	0.378	4.97	1.65	26.0	25.8	−0.7
SWB8L2	2.000	2.000	0.080	0.378	5.16	1.75	26.0	28.4	9.1
SWB8L3	2.000	2.000	0.080	0.378	5.12	1.90	26.6	30.3	13.9
DLE2A	2.250	2.250	0.060	0.420	4.28	1.00	13.4	13.6	1.6
DLE3	3.000	3.000	0.075	1.252	4.84	1.00	7.9	8.7	10.7
DLE4	3.000	3.000	0.075	1.252	4.79	1.00	8.5	8.6	1.6
DLE5	3.000	2.000	0.080	0.526	4.96	3.00	40.5	39.5	−2.6
SRC1	3.000	3.000	0.080	1.329	5.27	1.50	12.1	13.2	9.0
SRC2	3.000	3.000	0.080	1.329	5.24	1.50	12.5	13.1	5.3
5RC3	3.000	3.000	0.080	1.329	5.24	1.50	12.1	13.1	8.4
MWB-1A	3.000	3.000	0.075	1.252	5.32	3.00	24.6	26.0	5.8
	3.000	3.000	0.075	1.252	5.29	1.50	14.4	13.7	−4.6
MWB-2A	3.000	3.000	0.075	1.252	5.27	2.50	22.6	21.7	−3.9
	3.000	3.000	0.075	1.252	5.20	2.00	19.0	17.4	−8.2
MWB-3A	3.000	3.000	0.075	1.252	5.29	3.00	24.4	25.9	6.0
	3.000	3.000	0.075	1.252	5.26	3.00	23.6	25.7	9.0
MWB1	2.250	2.250	0.060	0.420	4.35	2.25	29.6	28.2	−4.7
	2.250	2.250	0.060	0.420	4.47	1.00	14.2	14.3	0.7
MWB2	2.250	2.250	0.060	0.420	4.30	2.25	30.4	27.8	−8.4
	2.250	2.250	0.060	0.420	4.47	1.50	21.6	20.2	−6.5
MWB3	2.250	2.250	0.060	0.420	4.38	2.25	29.3	28.5	−2.8
	2.250	2.250	0.060	0.420	4.41	2.25	29.8	28.6	−3.9
MWB3B	3.000	3.000	0.075	1.252	5.25	3.00	24.8	25.6	3.4
ST1	2.250	2.250	0.060	0.420	4.20	2.45	28.3	29.4	4.0
	2.250	2.250	0.060	0.420	4.45	2.40	29.0	30.7	5.7
ST2	2.250	2.250	0.060	0.420	4.21	2.40	28.1	28.9	3.0
	2.250	2.250	0.060	0.420	4.29	2.35	28.3	29.0	2.3
CAL-1A	2.250	2.250	0.060	0.420	4.38	1.13	15.4	15.4	0.3
CAL-1.5	2.250	2.250	0.060	0.420	4.58	1.63	22.8	22.3	−2.3
CAL-2	3.000	3.000	0.080	1.329	5.55	2.25	21.2	20.2	−5.0
CAL-2A	3.000	3.000	0.080	1.329	5.48	1.94	18.1	17.4	−4.1
CAL-2.5	3.000	3.000	0.080	1.329	5.35	2.56	20.4	21.9	7.3
POH1	3.000	3.000	0.080	1.329	5.12	2.92	23.3	23.6	1.4
SWBCAL2	3.000	3.000	0.083	1.375	4.22	2.50	18.0	16.3	−9.3
SWBCAL3	3.000	3.000	0.083	1.375	4.13	2.50	15.3	16.0	4.3
5WBCAL4	2.250	2.250	0.060	0.420	4.06	2.00	22.1	23.5	6.4
SWBCAL5	2.250	2.250	0.060	0.420	4.17	2.00	21.2	24.2	14.3
PT12	2.250	2.250	0.060	0.420	4.24	1.25	16.4	16.3	−0.9
	2.250	2.250	0.060	0.420	2.25	2.25	28.0	27.8	−0.8
PT23	3.000	3.000	0.083	1.375	6.35	2.20	20.8	22.4	7.9
	3.000	3.000	0.083	1.375	6.33	3.00	26.4	29.8	12.8

model represented by Equation 7 were considered. Both models used all 45 data points in calculating the empirical coefficients, and the t-test included model predictions for the same 45 data points. The first model is the one used to generate the predicted values of Table 2 and has a C_5 of 1.3123 $in.^2/kJ$ and a C_6 of 0.004042 $in.^5/kJ^2$. The second model assumes C_6 is zero (no second term in the model) before calculating C_5 using the least squares fitting procedure to all 45 data points. This model has a C_5 of 1.4404 $in.^2/kJ$.

Applying the paired t-test to the percent differences between the predictions and the data for both models resulted in a t value of 2.11. This value means that it can be said with 96% confidence that the value of C_6 is not equal to zero. Therefore, even though the numerical value of C_6 is much smaller than that of C_5, the confidence level that C_6 is not zero is high enough to justify keeping the C_6 term.

Effect of Beam Geometry and Weld Parameters on Weld Deflections

The control of weld deflections requires an understanding of how individual factors influence the deflections. Once verified, the model can be used to provide insight into the behavior of welded tubular beams. To examine the effect of a parameter on the weld deformations, the other parameters are held constant while the parameter of interest is varied. A graph of the weld deflection vs. the parameter of interest can then be drawn. The individual parameters examined in this study are the length of the weld (L), the heat input (H), the height of the tubular beam (h), the beam size, and the beam thickness (t).

Effect of Weld Length

The model and the data indicate that an increase in weld length increases the weld deflection. Figure 5A and 5B has been prepared to show the weld deflections as a function of weld length. Figure

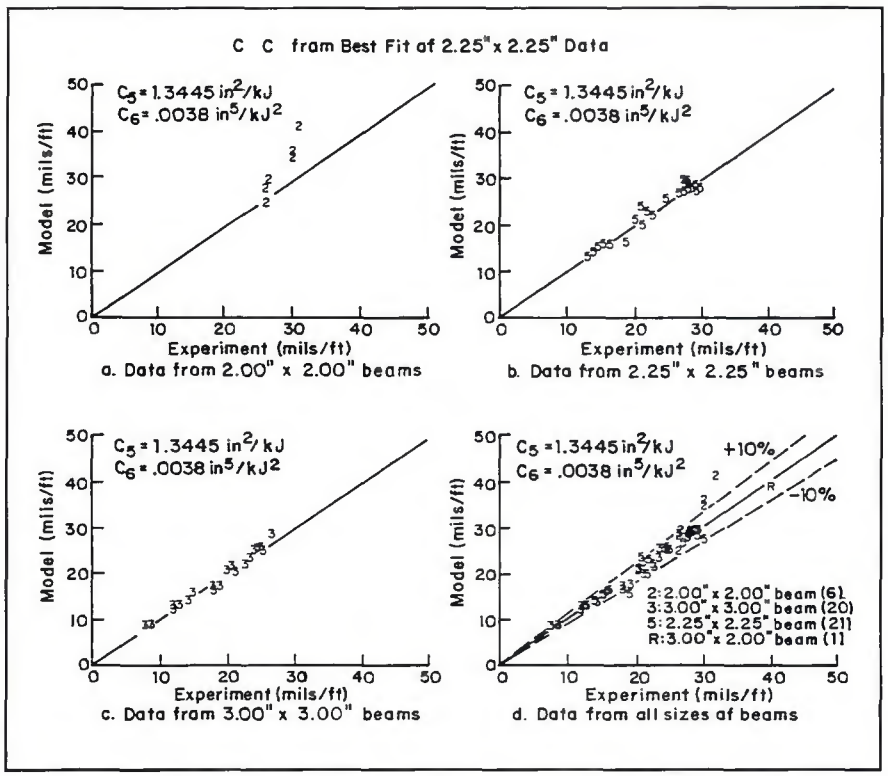

Fig. 3 — Comparison of predicted weld deflections and data for different beam sizes using coefficients based on 2.25 × 2.25-in. data.

5A is for the 2.25 × 2.25-in. beam with a wall thickness of 0.06 in. Figure 5B is for the 3 × 3-in. beam with a thickness of 0.075 in. Both figures identify the beams from which the data were taken. It appears from these data that the relation between the deflection and the weld length is essentially linear for both beam sizes.

It can be seen from Equation 7 that the model also predicts the weld deflection to be a linear function of weld length. Using C_5 and C_6 from fitting all of the data points (C_5 = 1.3123 in.²/kJ; C_6 = 0.004042 in.⁵/kJ²) and fixing heat input at 4.4 kJ/in., Equation 7 for the 2.25 × 2.25-in beam becomes:

$$\Delta\Theta = 2.57 + 22.37\ L \qquad (10)$$

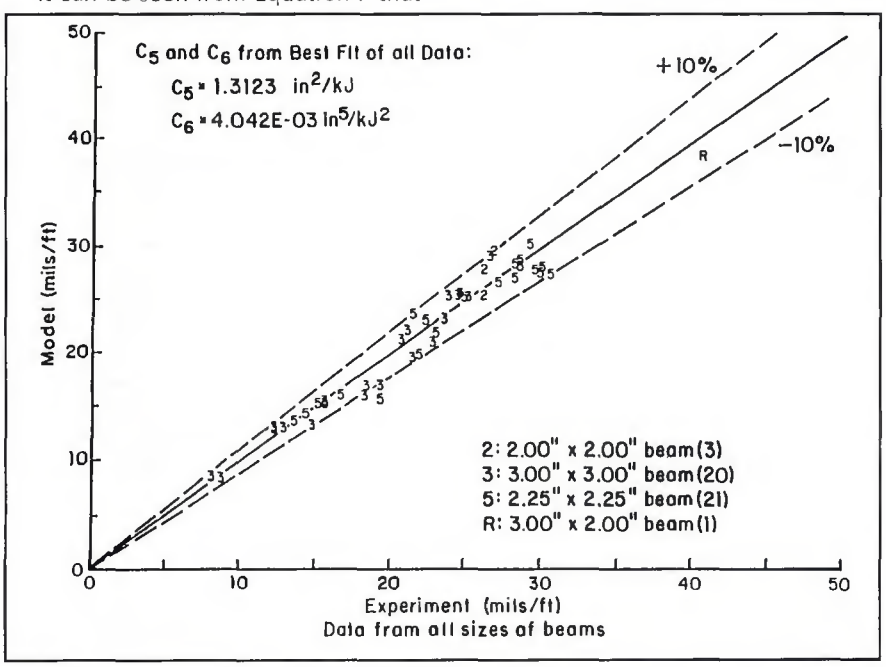

Fig. 4 — Comparison of weld deflections from model and data. Coefficients are based on fit of all data.

Using the same C_5 and C_6, a heat input of 5.3 kJ/in. and the 3 × 3-in. beam geometry, Equation 7 becomes

$$\Delta\Theta = 1.72 + 7.91\ L \qquad (11)$$

These equations are also plotted in Fig. 5A and 5B as model predictions. It can be seen from Fig. 5 that the data for both beam sizes are in good agreement with the proposed semiempirical model. It can also be seen that the constant terms in Equations 8 and 9 are important to providing a good fit to the data. Therefore, the term of Equation 7 with coefficient C_6 has a significant impact on the model even though the magnitude of C_6 is much smaller than C_5.

Effect of Heat Input

There is a range of practical heat inputs that can be used for a specific weld. The general understanding that increasing heat input increases the weld deflections is supported by the data and model presented in this study. Figure 6 combines predictions of the model and data to show the effect of heat input on the weld deflection. To isolate heat input as a welding parameter, data were selected for cases that maintained other parameters at constant values. For the 2.25 × 2.25 × 0.06-in. tubular beam, there are four data points with a weld length of 2-in. and heat inputs ranging from 2.76 kJ/in. to 4.40 kJ/in. The semiempirical model represented by Equation 7 assumes that the change in slope of the welded beam is proportional to heat input in the first term and proportional to heat input squared in the second term. However, the coefficient of the squared term is small; thus the model predicts a slightly nonlinear relation between the weld deflection and the heat inputs for the range of practical values used in this study. Figure 6A shows the effect of heat input for the 2.25-in. square beam. Figure 6B shows a similar plot for the 3-in. square beam. The thickness of this beam varies from 0.075 to 0.083 in. Data are available for a range of heat inputs for weld lengths of 2.5 in. The heat inputs range from 4.13 kJ/in. to 5.35 kJ/in. Because of the thickness range, the model was run for the minimum and maximum thicknesses. The curves in Fig. 6 are slightly nonlinear because the model indicates that the relation between the weld deflection and the heat input is slightly nonlinear for the heat input range of practical interest.

Effect of Beam Height

Beam height affects the moment of inertia, the moment arm (h/2), and D, in

Table 2 — Transverse Weld Deflection Data and Predicted Deflections from Model Using C5 and C6 from Best Fit of All Data

C5 = 1.3123 $in.^2/kJ$
C6 = 4.042E-03 $in.^5/kJ^2$

Specimen ID	Base (b) (in.)	Height (h) (in.)	Beam thick (in.)	Beam moment I	Heat input (kJ/in.)	Bead length (in.)	Exp. theta (mpft)	Model theta (mpft)	Diff (%)
SWB6L1	2.250	2.250	0.060	0.420	2.66	2.15	19.0	15.7	−17.3
SWB6L2	2.250	2.250	0.060	0.420	2.76	2.00	15.0	15.3	1.7
SWB6H1	2.250	2.250	0.060	0.420	4.40	2.00	25.0	25.3	1.1
SWB6H2	2.250	2.250	0.060	0.420	4.43	2.10	27.0	26.6	−1.4
SWB8L1	2.000	2.000	0.080	0.378	4.97	1.65	26.0	25.4	−2.2
SWB8L2	2.000	2.000	0.080	0.378	5.16	1.75	26.0	27.9	7.4
SWB8L3	2.000	2.000	0.080	0.378	5.12	1.90	26.6	29.8	12.0
DLE2A	2.250	2.250	0.060	0.420	4.28	1.00	13.4	13.5	0.6
DLE3	3.000	3.000	0.075	1.252	4.84	1.00	7.9	8.7	9.6
DLE4	3.000	3.000	0.075	1.252	4.79	1.00	8.5	8.5	0.5
DLE5	3.000	2.000	0.080	0.526	4.96	3.00	40.5	38.7	−4.4
SRC1	3.000	3.000	0.080	1.329	5.27	1.50	12.1	13.0	7.4
SRC2	3.000	3.000	0.080	1.329	5.24	1.50	12.5	12.9	3.7
SRC3	3.000	3.000	0.080	1.329	5.24	1.50	12.1	12.9	6.8
MWB-1A	3.000	3.000	0.075	1.252	5.32	3.00	24.6	25.6	3.9
	3.000	3.000	0.075	1.252	5.29	1.50	14.4	13.6	−5.9
MWB-2A	3.000	3.000	0.075	1.252	5.27	2.50	22.6	21.3	−5.6
	3.000	3.000	0.075	1.252	5.20	2.00	19.0	17.2	−9.7
MWB-3A	3.000	3.000	0.075	1.252	5.29	3.00	24.4	25.4	4.1
	3.000	3.000	0.075	1.252	5.26	3.00	23.6	25.3	7.0
MWB1	2.250	2.250	0.060	0.420	4.35	2.25	29.6	27.7	−6.3
	2.250	2.250	0.060	0.420	4.47	1.00	14.2	14.2	−0.2
MWB2	2.250	2.250	0.060	0.420	4.30	2.25	30.4	27.4	−9.9
	2.250	2.250	0.060	0.420	4.47	1.50	21.6	19.9	−7.7
MWB3	2.250	2.250	0.060	0.420	4.38	2.25	29.3	28.0	−4.4
	2.250	2.250	0.060	0.420	4.41	2.25	29.8	28.2	−5.5
MWB3B	3.000	3.000	0.075	1.252	5.25	3.00	24.8	25.2	1.5
ST1	2.250	2.250	0.060	0.420	4.20	2.45	28.3	28.9	2.2
	2.250	2.250	0.060	0.420	4.45	2.40	29.0	30.1	4.0
ST2	2.250	2.250	0.060	0.420	4.21	2.40	28.1	28.4	1.2
	2.250	2.250	0.060	0.420	4.29	2.35	28.3	28.5	0.6
CAL-1A	2.250	2.250	0.060	0.420	4.38	1.13	15.4	15.3	−0.7
CAL-1.5	2.250	2.250	0.060	0.420	4.58	1.63	22.8	22.0	−3.7
CAL-2	3.000	3.000	0.080	1.329	5.55	2.25	21.2	19.8	−6.6
CAL-2A	3.000	3.000	0.080	1.329	5.48	1.94	18.1	17.1	−5.6
CAL-2.5	3.000	3.000	0.080	1.329	5.35	2.56	20.4	21.5	5.4
POH1	3.000	3.000	0.080	1.329	5.12	2.92	23.3	23.2	−0.5
SWBCAL2	3.000	3.000	0.083	1.375	4.22	2.50	18.0	16.0	−11.1
SWBCAL3	3.000	3.000	0.083	1.375	4.13	2.50	15.3	15.7	−2.3
SWBCAL4	2.250	2.250	0.060	0.420	4.06	2.00	22.1	23.1	4.6
SWBCAL5	2.250	2.250	0.060	0.420	4.17	2.00	21.2	23.8	12.4
PT12	2.250	2.250	0.060	0.420	4.24	1.25	16.4	16.1	−2.1
	2.250	2.250	0.060	0.420	4.28	2.25	28.0	27.3	−2.5
PT23	3.000	3.000	0.083	1.375	6.35	2.20	20.8	22.1	6.2
	3.000	3.000	0.083	1.375	6.33	3.00	26.4	29.2	10.8

Equation 7. An increase in beam height increases the moment of inertia as h^3, while the numerator of Equation 7 increases only as $h^{1.5}$. Thus, an increase in beam height tends to decrease the weld deflection. This behavior is illustrated in Fig. 7.

For this figure, the base, b, and the weld length, L, are held constant at 3 in. The thickness is 0.075 in. All data and model predictions except that of DLE5-1 have a thickness of 0.080 in. The heat inputs for the four data points range from 4.96 kJ/in. to 5.32 kJ/in., so the model was run for these two heat input values to show the effect of this variation.

Figure 7 shows a nonlinear effect of beam height on the weld deflections. Again, the data show good agreement with the predicted deflections of the model. The nonlinear effect of halving the beam height from 3 to 1.5 in. more than doubles the deflections from 24 mils/ft to 60 mils/ft. Thus, it can be seen that the beam height has a large effect on the deflections of the welded beam when the base dimension and the weld length are kept constant.

Effect of Beam Size on Weld Deflections

It is useful to design engineers to have an understanding of how the weld deflections are influenced by the size of the beam. To illustrate the effect of beam size on weld induced deflections, a series of analyses were done using square beams (b=h). Two sets of heat inputs and wall thicknesses were selected based on values from available data. The beam height was varied from 1.0 to 4.0 in. Figure 8 shows that the weld deflection decreases for increasing beam size. Comparing the curve in Figure 8 with that in Fig. 7, it can be seen that deflections are somewhat more sensitive to beam height. One factor contributing to this difference is that the weld length is constant for the cases shown in Fig. 7, while the weld length is increasing with beam size for the cases shown in Fig. 8. There is good agreement between the trends of the model and the data of Fig. 8.

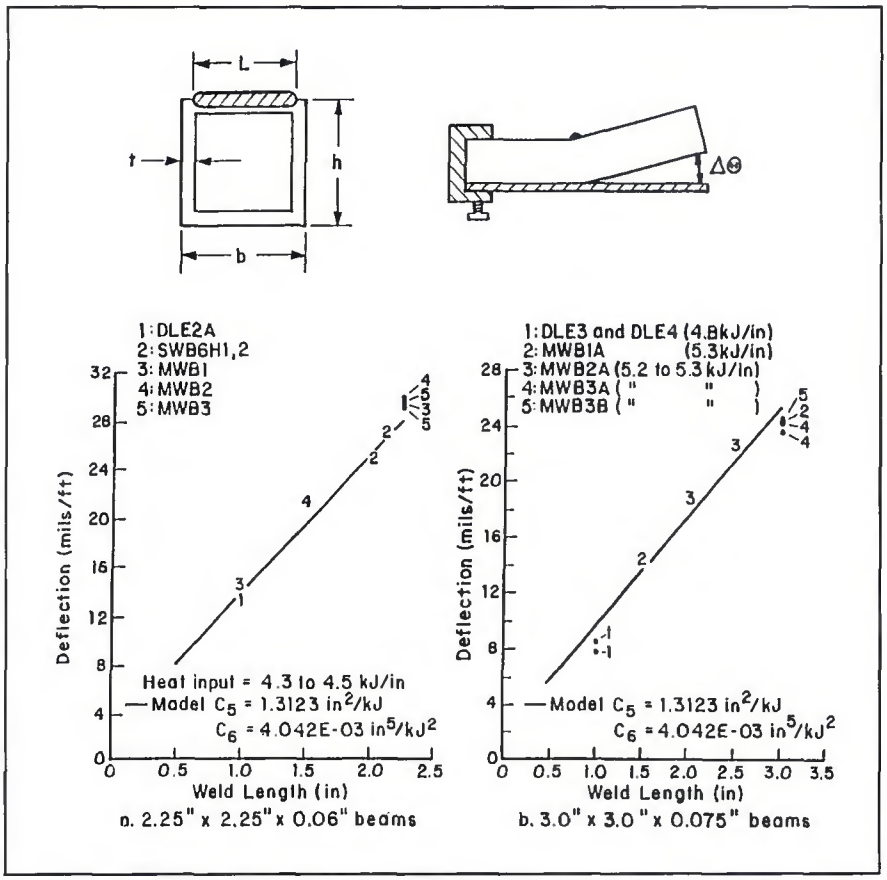

Fig. 5 — Effect of weld length on deflections. Experimental and predicted values for two beam sizes.

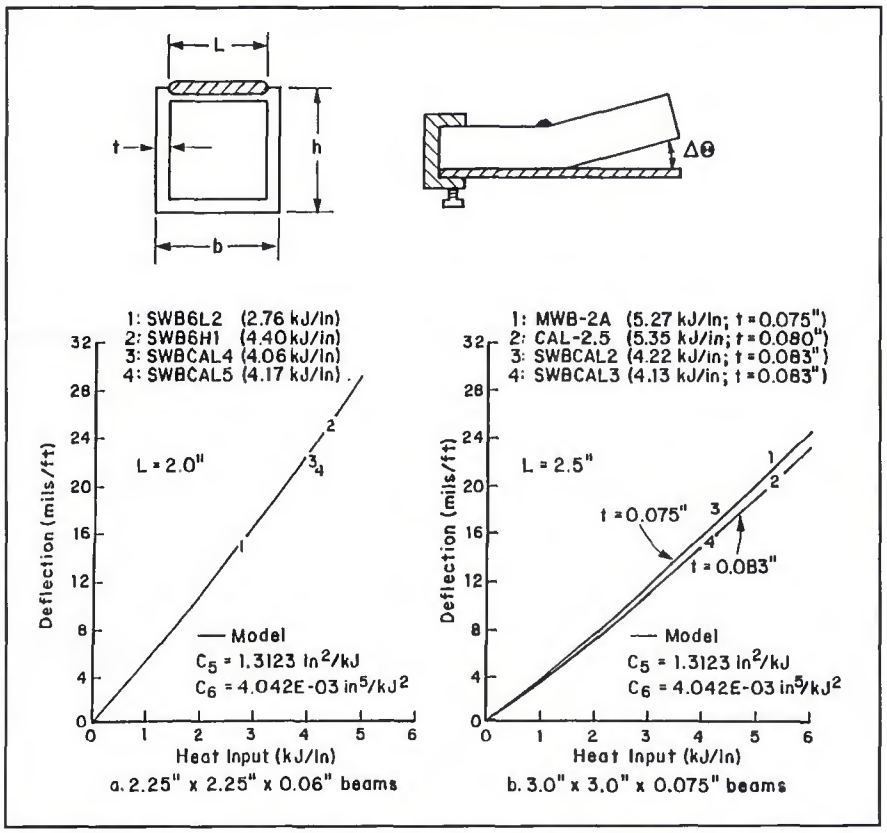

Fig. 6 — Effect of heat input on weld deflections: data and model predictions.

Effect of Beam Thickness on Weld Deflections

The beam wall thickness, t, influences the moment of inertia, I, and also the numerator of the first term of Equation 7. The moment of inertia varies as t^3, while the numerator varies as $t^{1/2}$. Thus, the overall effect is a decrease in the weld deflection for thicker beams.

Figure 9 illustrates the effect of beam thickness for thicknesses ranging from 0.04 to 0.09 in. Beam sizes of 3 × 3 and 3 × 2 in. were chosen with heat inputs representative of those used in the experiments. The weld length was assumed equal to the base of the beam (3 in.). As expected, the model shows a decrease in weld deflection for increasing thickness. For the 3 × 3 in. beam, an increase in thickness from 0.04 to 0.08 in. decreases the weld deflection from 35 to 24 mils/ft. The two data points in Fig. 9 are close to the curves generated by the model.

Summary and Conclusions

A model to represent the deflections due to transverse welds on thin-walled tubular beams is presented. The model is semi-empirical and simple enough to be programmed on a personal computer using spreadsheet software. An initial evaluation of the model was done by calculating the two empirical coefficients using data for one square beam size. The model was then used to predict the weld deflections for two other square beam sizes and one rectangular beam. The agreement between the model and the data was generally better than 10%. The two empirical coefficients, C_5 and C_6, were then obtained by fitting the model to all available data. The resulting C_5 was within 2% of the previously computed value and the C_6 was within 6%. The overall agreement with the data was largely unchanged.

The model and the data were used to examine the effect of weld and geometric parameters on weld deflections. The weld parameters which were considered were weld length, L, and heat input, H. Geometric parameters included beam height, (h), beam size for square beam (b=h), and wall thickness (t). Results of the model and data showed that the weld deflections were proportional to the weld length and essentially proportional to the heat input. The height of the beam affects the moment of inertia and the moment arm of the weld residual stresses. The result was a nonlinear relation between the weld deflection and the height of the beam. Thus, decreasing the beam height by half more than doubles the weld deflection. It was also shown that deflections for

typical welds on square beams can be significantly larger for smaller beam sizes. While results showed that deflections tend to increase with a decrease in beam thickness, the deflections are less sensitive to changes in beam thickness than to changes in beam height or beam size.

The proposed model is a simple computational tool for the prediction of weld deflections due to transverse welds on thin-walled square beams. The model shows promise as a tool for predicting the effects of heat input, weld length, beam height, size and thickness on the deflections caused by transverse gas metal arc welds. It should be pointed out that while the model showed good agreement with the data for the cases presented here, the model should not be applied outside the range of parameters for which it has been tested. In particular, the model was developed for square beams made of a specific material and only a limited range of heat inputs and thicknesses were considered. Further development of the model is recommended before applications are extended to rectangular or other geometric cross-sections or to other materials and heat inputs. Concerning applications of this model to different materials, it is noted that the terms C_1 and C_2 of Equations 3 and 5, and hence C_5 and C_6 of Equation 7, depend on the material properties of the system. Specifically, if a different material system is of interest, the values of the empirical parameters, C_5 and C_6, must be determined from weld deflection data for the new material. Therefore, applications to other materials should be preceded by verification studies and tests to determine the appropriate empirical values of these parameters.

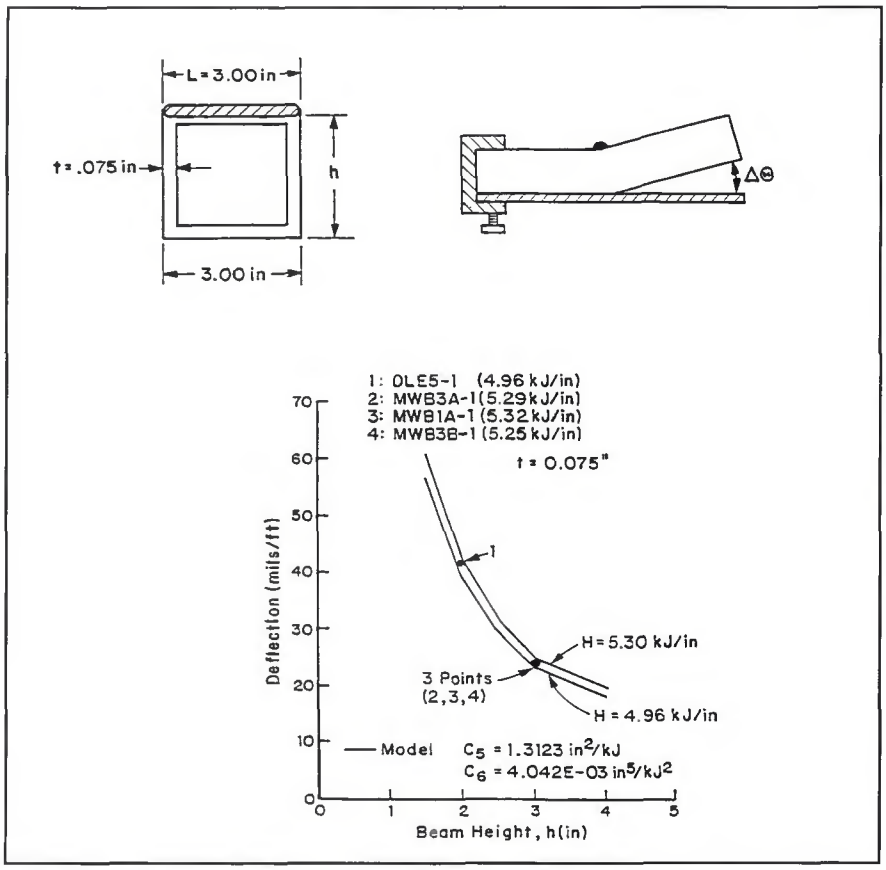

Fig. 7 — Effect of beam height on weld deflections: data and model predictions.

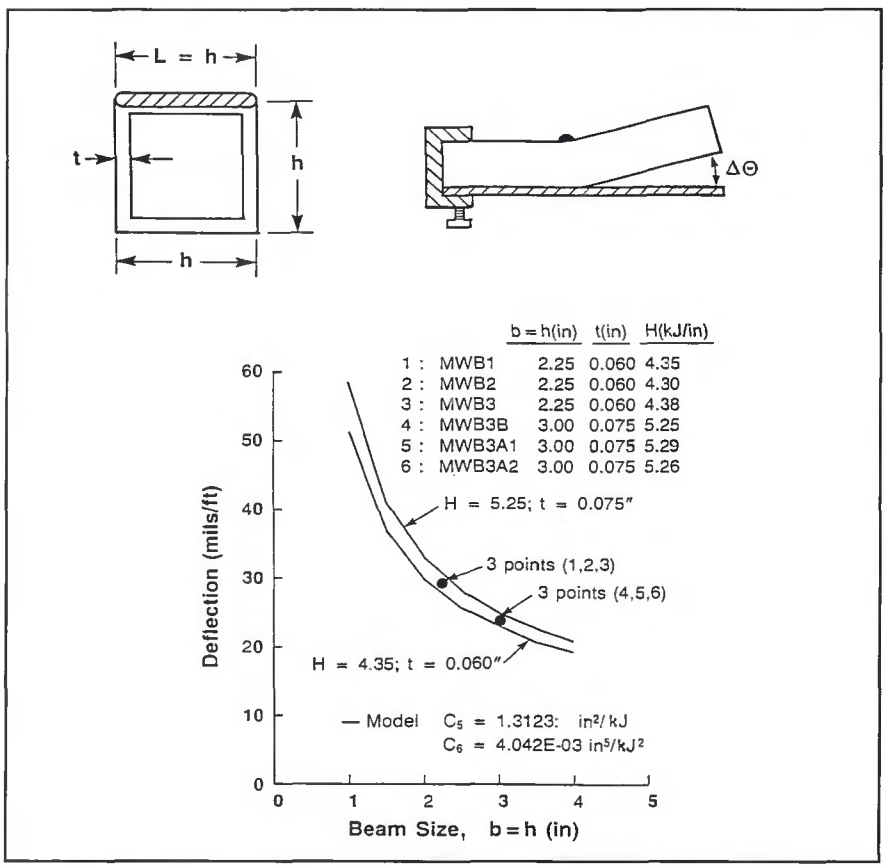

Fig. 8 — Effect of beam size on weld deflections.

References

1. Masubuchi, K., Analysis of Welded Structures, Pergaman Press, New York, 1980, Chapter 7.

2. Masubuchi, K., "Research Activities Examine Residual Stresses and Distortion in Welded Structures," *Welding Journal*, December 1991, pp. 41–47.

3. Arya, S. K., and Paramar, R. S., "Mathematical Models for Predicting Angular Distortion in CO_2-Shielded Flux Cored Arc Welding," *Proceedings of the International Conference on Joining of Metals* held in Helsinger, Denmark, Dec. 19–22,1986, Vol. 3, pp. 240–245.

4. Kjaersgaard, C. J., Terndrup-Larsen, T., and Nielsen, K., "Welding Distortions Resulting from Flux Cored Arc Welding," *Proceedings of the Conference on the Joining of Materials* held in Helsinger, Denmark, May 10–12,1989, Vol. 5, pp. 142–149.

5. Ueda, Y., Nakacho, K., and Moriyama, S., "Simple Prediction Methods for Welding Deflection and Residual Stress of Stiffened

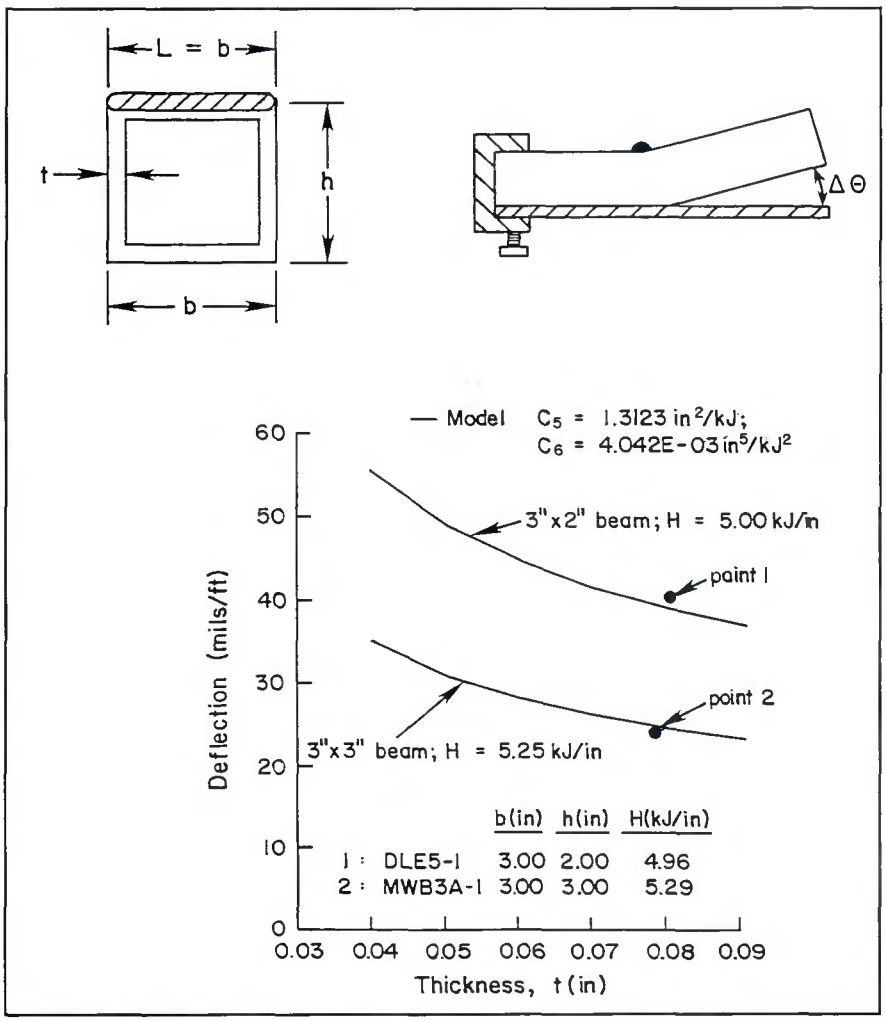

Fig. 9 — Effect of beam thickness on weld deflections: data and model predictions.

Panels," *Transactions of the Japan Welding Research Institute*, Vol. 15, Num. 2, Dec. 1986, pp. 369–376.

6. Tekriwal, P., and Mazumder, J., "Transient and Residual Thermal Strain-Stress Analysis of GMAW," *Journal of Engineering Materials and Technology*, Vol. 113, July 1991, pp. 336–343.

7. Iwamura, Y., and Rybicki, E. F., "A Transient Elastic Plastic Thermal Stress Analysis for Flame Forming," *Journal of Engineering for Industry*, Transactions of the ASME, Feb. 1973, pp. 163–171.

8. Rybicki, E. F., Stonesifer, R. B., Merrick, E. A., and Haueter, J. R., "A Computational and Experimental Study of Deformations in a Draw Bead Welded Pipe," *Welding Journal*, April 1986, pp. 99s–105s.

9. Hou, Chien-ann, "Modeling and Control of Welding Distortion in Tubular Frame Structures," Ph.D. Dissertation, Ohio State University, Dissertation Advisors: C. L. Tsai and G. L. Kinzel, 1986.